Stabilizing and Destabilizing Effects of Placing β-Branched Amino Acids in Protein α-Helices†

Virginia W. Cornish,‡ Mark I. Kaplan,§ David L. Veenstra,∥ Peter A. Kollman,∥ and Peter G. Schultz*,‡

Department of Chemistry, University of California, Berkeley, California 94720, and Graduate Group in Biophysics and Department of Pharmaceutical Chemistry, University of California, San Francisco, California 94143

Received May 3, 1994; Revised Manuscript Received July 25, 1994®

ABSTRACT: In order to gain greater insight into the effects of β-branched amino acids on protein α-helices, hydrophobic amino acids with varying degrees of β-branching, including the fully β-substituted L-2-amino-3,3-dimethylbutanoic acid (ADBA), were incorporated into the protein T4 lysozyme. The unnatural and natural amino acids were substituted at two solvent-exposed α-helical sites, Ser 44 and Asn 68, in the protein using the technique of unnatural amino acid mutagenesis. The stabilities of the mutant proteins were determined by using a heat of inactivation assay and from their circular dichroism thermal denaturation curves. Surprisingly, while substitution of the amino acid with the greatest degree of β-branching, ADBA, destabilizes the protein by 2.5 ± 0.1 °C (0.69 ± 0.03 kcal/mol) relative to Ala at site 44, the same substitution *stabilizes* the protein by 1.0 ± 0.1 °C (0.27 ± 0.03 kcal/mol) at site 68. The difference observed at these two positions illustrates the extent to which the local context can mediate the impact of a particular mutation. Molecular dynamics simulations were carried out in parallel to model the structures of the mutant proteins and to examine the energetic consequences of incorporating ADBA. Together, these results suggest that the conformationally restricted β-branched amino acids are destabilizing, in part, because the β-branched methyl groups can cause distortions in the local helix backbone. In addition, it is proposed that in some contexts the conformational rigidity of β-branched amino acids may be stabilizing because it lowers the entropic cost of forming favorable side-chain van der Waals interactions.

In trying to understand the forces that dictate protein structure, much work has focused on protein secondary structure (Creighton, 1990; Dill, 1990; Matthews, 1993). Regular secondary structure comprises about 50% of known protein structure (Dill, 1990), and recent evidence suggests that intermediates along several protein folding pathways contain elements of native secondary structure (Kim & Baldwin, 1990). Several approaches have been taken to determine which amino acids stabilize α-helices and promote α-helix formation. Statistical surveys of protein structures reveal that certain amino acids are found in α-helices more frequently than others (Chou & Fasman, 1978; Richardson & Richardson, 1988; Williams et al., 1987). In early experimental work the Zimm–Bragg parameters for helix nucleation (σ) and propagation (s) were determined for the 20 natural amino acids using random copolymers containing a "host" amino acid and different "guest" amino acids (Scholtz et al., 1991; Scheraga, 1978; Sueki et al., 1984; Wojcik et al., 1990; Zimm & Bragg, 1959). More recently, model peptides designed to adopt α-helical structures in solution have been used to assess the helix-forming propensities of different amino acids (Lyu et al., 1990; Marqusee et al., 1989; Merutka et al., 1990; O'Neil & DeGrado, 1990; Padmanabhan et al., 1990; Zhou et al., 1993). Similarly, the helix-forming tendencies of the natural amino acids have been evaluated by substituting all of the natural amino acids at a single α-helical position in a protein and then determining the effect of these mutations on the protein's stability (Blaber et al., 1993, 1994; Horovitz et al., 1992; Serrano et al., 1992a,b). In addition, theoretical calculations have been used both to estimate the helix-promoting abilities of different amino acids and to develop models for why a particular amino acid may stabilize an α-helix (Hermans et al., 1992). On the basis of this work, certain amino acids have been suggested to promote α-helix formation, while others have been suggested to disrupt α-helix formation.

In particular, the naturally occurring β-branched amino acids valine, isoleucine, and threonine appear to destabilize α-helices in both proteins and peptides. In order to gain a more precise estimate of the impact of β-branched side chains on α-helix stability, Lyu et al. substituted a series of β-branched and linear hydrophobic amino acids at position Xaa in the model peptide Ac-Tyr-Ser-Glu_4-Lys_4-Xaa_3-Glu_4-Lys_4-NH_2 (Lyu et al., 1991). While peptides containing amino acids bearing linear side chains (e.g., methyl, ethyl, *n*-propyl, *n*-butyl) were all roughly equal in α-helical content, peptides containing amino acids with isopropyl and *tert*-butyl side chains were significantly less helical. Since peptides containing linear and γ-branched amino acids had similar α-helical content, the destabilizing effect of the other amino acids was attributed to the β-branching. Indeed, Lyu et al. observed a linear relationship between the addition of β-branched methyl groups to a linear amino acid side chain and the decrease in the peptide's helical content; they estimated that each β-branched methyl group decreased the stability of the helical peptide by 0.45 kcal/mol. Theoretical work by Hermans and co-workers on the projected stability of an alanine-based helix containing a similar set of β-branched amino acids also predicted that β-branched side chains should destabilize α-helices, although the destabilization was predicted to be slightly greater (Hermans et al., 1992).

† This work was supported by grants from the NIH (GM49220 to P.G.S. and GM29072 to P.A.K), an NSF predoctoral fellowship to V.W.C., an ONR fellowship to M.I.K., and a Glaxo fellowship to D.L.V.

* Author to whom correspondence should be addressed.

‡ Department of Chemistry, University of California, Berkeley.

§ Graduate Group in Biophysics, University of California, San Francisco.

∥ Department of Pharmaceutical Chemistry, University of California, San Francisco.

® Abstract published in *Advance ACS Abstracts,* September 15, 1994.

0006-2960/94/0433-12022$04.50/0

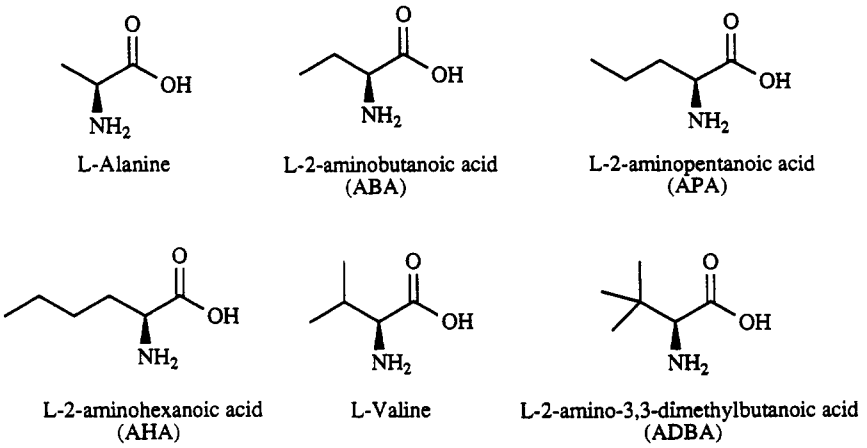

FIGURE 1: Amino acids substituted at sites Ser 44 and Asn 68.

In order to probe whether the effects of β-branching in protein α-helices are similar to those in peptide model systems, we determined the thermal stability of T4 lysozyme (T4L) mutants containing a similar series of β-branched and linear amino acids (Figure 1) substituted at two different sites, Ser 44 and Asn 68, both of which lie at solvent-exposed positions in the middle of α-helices in T4L (Remington et al., 1978; Weaver & Matthews, 1987). The mutant proteins were prepared using the technique of unnatural amino acid mutagenesis (Bain et al., 1989; Ellman et al., 1992a; Noren et al., 1989). The stabilities of mutant proteins containing the amino acids alanine, L-2-aminobutanoic acid (ABA), valine, L-2-aminopentanoic acid (APA), L-2-amino-3,3-dimethylbutanoic acid (ADBA), and L-2-aminohexanoic acid (AHA) were measured using a heat of inactivation assay (Matthews et al., 1987; Wells & Powers, 1986). Mutants containing ADBA were then examined in detail because in this amino acid all β-hydrogens are replaced with methyl groups, and so this amino acid should display the most pronounced effects; AHA and Ala were included as controls. The mutant proteins were purified to homogeneity, and their stabilities were characterized by monitoring their thermal denaturation using circular dichroism spectroscopy (Becktel & Baase, 1987). Molecular dynamics simulations of the mutant proteins were carried out in parallel in order to gain additional insights into the effects of these mutations.

EXPERIMENTAL PROCEDURES

Materials. Restriction enzymes were purchased from New England Biolabs; T4 DNA ligase was from Promega; reagents and enzymes for DNA mutagenesis and sequencing were obtained from Amersham and U.S. Biochemicals, respectively. Oligonucleotides were synthesized on an Applied Biosystems PCR Mate DNA synthesizer. All chemicals were purchased from Sigma or Aldrich. NMR spectra were recorded on the UCB-400 (400 MHz) or the UCB-500 (500 MHz) Fourier transform NMR spectrometers at the University of California, Berkeley, NMR facility. The internal standard for ^{1}H NMR spectra determined in $CDCl_3$ was Me_4Si and in DMSO-d_6 was the solvent (δ 2.49). All ^{13}C NMR spectra were proton decoupled and used solvent as the internal standard, $CDCl_3$ (δ 77.0) and DMSO (δ 39.5). Fast atom bombardment mass spectra were recorded at the University of California, Berkeley, mass spectral laboratory, with *m*-nitrobenzyl alcohol as the matrix solvent. High-pressure liquid chromatography (HPLC) was performed on a Waters Model 600E instrument using a Waters 490E UV detector and a Waters 745 data module. A Porasil column (M20 10/50 ODS-3) was used for preparative chromatography, and a Rainin C18 column (80-225-C15) was used for analytical chromatography. Thin-layer chromatography (TLC) was performed on silica gel (Merck Fertigplatten, 60F-254, Article 5765). All column chromatography was flash chromatography carried out on silica gel (Merck Kieselgel 60, Article 9385).

Mutant Lysozymes. Mutant proteins were constructed by Eckstein mutagenesis (Sayers et al., 1988) using an M13mp18 derivative containing a 650 base pair (bp) *Bam*HI/*Hin*dIII fragment that encodes a cysteine-free T4L behind a twin tac promoter from plasmid *pHSe54,97.TA* (Perry & Wetzel, 1987). The oligonucleotides 5′-AGC-TTT-ATC-TAA-TTC-CTA-TTT-AGC-AGC, 5′-AGC-TTT-ATC-TAA-TTC-TGC-TTT-AGC-AGC, 5′-ATC-AAC-ATC-CTG-CTA-AAA-GAG-TTT-TTC, and 5′-ATC-AAC-ATC-CTG-TGC-AAA-GAG-TTT-TTC were used to generate the *pTL44am*, *pT4L44A*, *pT4L68am*, and *pT4L68A* mutants, respectively. Mutations in the M13mp18 construct were verified by dideoxy sequencing (Sanger et al., 1977), and the entire T4L gene in *pHSe54,97.TA* was sequenced for all mutants.

General Procedure for the Formation of 6-Nitroveratryloxycarbonyl- (NVOC-) Protected Amino Acids (Robertson et al., 1991). The amino acid (2.4 mmol) and sodium carbonate (2.5 mmol) were dissolved in doubly distilled H_2O (20 mL). The protecting group NVOC-Cl (2.5 mmol) was dissolved in dioxane (20 mL) by heating the solution to 50 °C. Upon dissolution, the two solutions were combined, and the mixture was stirred from 2 to 12 h at room temperature (RT). The reaction was judged complete by thin-layer chromatography (TLC) using 98:2 ethyl acetate/hexane. The reaction mixture was then diluted with 1 N NaOH (20 mL) and extracted with CH_2Cl_2 (2×, 50 mL). The aqueous layer was acidified to pH 4 using 1 N citric acid or 1 N $NaHSO_4$ (ca. 25 mL) and extracted with ethyl acetate (3×, 100 mL). The organic extracts were combined, dried, and evaporated to afford the crude *N*-NVOC-protected amino acid which was carried on without further purification.

General Procedure for the Formation of Cyanomethyl Esters from N-Blocked Amino Acids (Robertson et al., 1991). The *N*-protected amino acid (0.39 mmol), triethylamine (0.85 mmol), and chloroacetonitrile (1.6 mmol) were stirred at RT overnight. The reaction was judged complete by TLC using a 1:1 ethyl acetate/hexane. The reaction mixture was then diluted with CH_2Cl_2 (20 mL) and extracted with 1 N $NaHSO_4$ (2×, 20 mL). The organic extract was dried, and the solvent was removed *in vacuo*. The product was purified by silica gel chromatography using 1:2 ethyl acetate/hexane followed by 1:1 ethyl acetate/hexane.

N-NVOC-L-2-aminohexanoate Cyanomethyl Ester. The derivatized amino acid was prepared as described in 63% overall yield to give a yellow solid: R_f = 0.18 in 1:2 ethyl acetate/hexane; ^{1}H NMR (400 MHz, $CDCl_3$) δ 7.69 (s, 1), 6.96 (s, 1), 5.57 (d, J = 15 Hz, 1), 5.44 (d, J = 15 Hz, 1), 5.32 (d, J = 8.2 Hz, 1), 4.82 (d, J = 16 Hz, 1), 4.69 (d, J = 16 Hz, 1), 4.40 (m, 1), 3.98 (s, 3), 3.93 (s, 3), 1.87 (m, 1), 1.70 (m, 1), 1.34 (m, 4), 0.89 (t, J = 6.9 Hz, 3); ^{13}C NMR (100 MHz, $CDCl_3$) δ 171.33, 155.43, 153.62, 148.14, 139.64, 127.71, 113.80, 109.87, 108.16, 63.97, 56.42, 56.34, 53.69, 48.88, 31.59, 27.32, 22.05, 13.67; MS, m/e 410.1 (MH^+). C, H, N analysis: calculated, C, 52.81%, H, 5.66%, N, 10.26%; found, C, 53.09%, H, 5.69%, N, 10.24%.

N-NVOC-L-2-amino-3,3-dimethylbutanoate Cyanomethyl Ester. The derivatized amino acid was prepared as described in 73% overall yield to give a yellow solid: R_f = 0.21 in 1:2 ethyl acetate/hexane; ^{1}H NMR (400 MHz, $CDCl_3$) δ 7.69 (s, 1), 6.95 (s, 1), 5.53 (d, J = 15 Hz, 1), 5.48 (d, J = 15 Hz, 1), 5.40 (d, J = 9.3 Hz, 1), 4.84 (d, J = 16 Hz, 1), 4.66 (d, J = 16 Hz, 1), 4.23 (d, J = 9.3 Hz, 1), 3.97 (s, 3), 3.93 (s, 3), 1.02 (s, 9); ^{13}C NMR (100 MHz, $CDCl_3$) δ 170.41, 155.60, 153.59, 148.24, 139.81, 127.54, 113.75, 110.10, 108.24, 64.04, 62.08, 56.42, 56.37, 48.42, 34.74, 26.41; MS, m/e 410.1 (MH^+); HR MS, calculated 409.149, found 409.149 (M).

General Procedure for the Aminoacylation of pdCpA Using N-NVOC-Protected Amino Acid Cyanomethyl Esters (Robertson et al., 1991). The *N*-protected amino acid cyanomethyl ester (0.50 mmol), tetrabutylammonium pdCpA (0.10 mmol), and dimethylformamide (1.4 mL) were stirred 2–12 h at RT in a dry vial. The reaction was judged complete by analytical HPLC using a linear gradient of 10:90 to 90:10 CH_3CN/50 mM NH_4OAc, pH 4.5, over 50 min. The desired, monoacylated product was purified by preparation HPLC using the same gradient, but over 90 min. Salt was removed from the purified product by preparative HPLC using a gradient of 10:90 to 90:10 CH_3CN/10 and mM HOAc over 90 min. Yields for the aminoacyl-pdCpA compounds were 40–60%. The pure product was stored as a solution of −80 °C and lyophilized prior to ligation to $tRNA^{Phe}_{CUA}$(−CA).

5′-Phospho-2′-deoxycytidylyl(3′–5′)-2′(3′)-O-(N-NVOC-L-2-aminohexanoyl)adenosine: MS, m/e 989.0 (MH^+); HR MS, calculated 989.244, found 989.244 (MH^+).

5′-Phospho-2′-deoxycytidylyl(3′–5′)-2′(3′)-O-(N-NVOC-L-2-amino-3,3-dimethylbutanoyl)adenosine: MS, m/e 989.0 (MH^+); HR MS, calculated 989.244, found 989.244 (MH^+).

In Vitro Protein Synthesis. Small-scale *in vitro* reactions, 30-μL final volume, were run as reported (Ellman et al., 1992a). Large-scale *in vitro* reactions, 5-mL final volume, were run similarly to small-scale reactions with the following modifications. After ligation of the aminoacyl-pdCpA (4.92 × 10^{-6} mol) to $tRNA^{Phe}_{CUA}$(-CA) (1.67 mg), the reaction was quenched by addition of 2.2 M sodium acetate (pH 4.5) to 25% (v/v) and precipitated with 2 volumes of ethanol on dry ice for at least 1 h. The aminoacyl-tRNA was pelleted by centrifugation at 12 × 10^3 rpm, 4 °C, for 20 min. The pellet was rinsed with cold 70% ethanol (10 mL) and then reprecipitated using the same conditions to ensure removal of unligated aminoacyl-pdCpA. The pellet was dried *in vacuo* for ca. 10 min, resuspended in 1 mM potassium acetate, pH 4.5, at 0.5 mg/mL, photodeprotected in two portions for 45 min each time, and stored at −80 °C until addition to the *in vitro* reaction. Plasmid (0.5 mg), $Mg(OAc)_2$ (5–7 mM), and LM mix (1.25 mL) were combined in a 50-mL sterile conical tube, DEPC-treated doubly distilled H_2O was added to 2.76 mL, and the mixture was preincubated at 37 °C for 5 min with shaking. After the temperature was equilibrated, the S-30 extract (1.4 mL) and the aminoacyl-tRNA solution (0.84 mL) were added rapidly, the reaction mixture was vortexed gently, and the reaction mixture was incubated at 37 °C for 1 h with shaking.

Purification of T4 Lysozyme. T4L was synthesized *in vitro* (20–40 μg of wild-type protein/mL of *in vitro* reaction mixture) and purified to homogeneity in 5–10% overall yield. The protein was purified as reported (Cornish et al., 1994), except that the final step of purification, passage over a Mono S column, was modified. The CM fractions containing T4L activity (2–8 mL) were combined and dialyzed for at least 4 h against two 500-mL portions of 50 mM Na_2HPO_4, pH 6.5, and 1 mM EDTA buffer (phosphate buffer). The solution was applied to a Mono S column (HR 5/5, Pharmacia) equilibrated in the phosphate buffer. The protein was eluted by using a Pharmacia FPLC with a 14-mL linear gradient of 0–0.5 M NaCl in the phosphate buffer at a flow rate of 0.5 mL/min, and 0.3-mL fractions were collected. Fractions containing T4L were identified by the absorbance at 280 nm and by catalytic activity. Protein yields were determined by SDS–PAGE with silver staining.

Heat of Inactivation. The stability of the T4L mutants was judged by measuring the activity of the proteins as a function of temperature (Ellman et al., 1992b; Matthews et al., 1987; Wells et al., 1986; Streisinger, 1968). Crude supernatants (30 μL) from terminated 120-μL *in vitro* reactions were diluted to 600 μL at a final buffer concentration of 100 mM NaCl, 200 mM Na_2HPO_4, pH 6.5, and 1 mM EDTA. The solution was divided into 50-μL portions, and each portion was heated for 10.0 min at a given temperature and then stored on ice at 4 °C. Each protein was assayed between 50 to 60 °C in 1.0 ± 0.1 °C increments. The residual activity for each portion was determined by measuring the rate of lysis of NAP IV cells. Each mutant protein was measured in triplicate, and the error in the T_m (the temperature at which the residual activity is 50%) was between 0.1 and 0.7 °C. All mutant proteins were judged to be intact structurally because the catalytic activity as measured by the rate of NAP IV cell-wall lysis agreed with the quantity of protein as determined by SDS–PAGE and autoradiography. The specific activity cannot be determined for T4L because the only substrate toward which the protein is active is the cell wall.

Thermal Stability. The stability of purified T4L mutants was determined by monitoring the thermal denaturation of the protein by using circular dichroism spectrometry (Becktel et al., 1987). Purified proteins were dialyzed in a Pierce microdialyzer, fitted with a membrane with a MWCO of ca. 12 kDa, against eight 120-mL changes of 20 mM K_2HPO_4, pH 2.5, and 25 mM KCl buffer over 12 h at RT. The buffer was prepared as reported by Sturtevant—20 mM in K_2HPO_4 and 25 mM in KCl—and the pH was adjusted to 2.5 with HCl (Kutamura & Sturtevant, 1989). The CD wavelength scans and melting curves were measured on an AVIV Model 62DS circular dichroism spectrometer equipped with an AVIV thermoelectric temperature controller and a thermostatically controlled cuvette holder. For the wavelength scans, the CD spectra of the proteins were recorded from 200 to 260 nm, every 1 nm, at 20.0 °C, and data were acquired at each wavelength for 5.0 s. All of the purified proteins showed minima at 209 and 223 nm and had spectra similar to that of wild type (data not shown). Molar ellipticity is not reported as the exact concentration of the protein solutions was not determined. For the thermal melts, the ellipticity at 223 nm

was monitored at 1.0 °C temperature increments from 20.0 to 65.0 °C. The sample was equilibrated at each temperature for 60 s, and data were acquired at each temperature for 60 s. After each melt, the sample temperature was returned to 20 °C, and the θ_{223} was determined to be at least 80% of the original value. The thermal denaturation curve for each mutant was measured twice using the same sample each time. The T_m for each protein was determined from its melting curve using nonlinear regression analysis as described (Santoro & Bolen, 1992). The calculated T_m correlates to the mean value of the two T_ms determined from independent melts, and the error reported is the standard deviation between these two values. The $\Delta\Delta G(\Delta G_{Ala} - \Delta G_{mut})$ for each protein was calculated from the ΔT_m ($T_{m,mutant} - T_{m,Ala}$) using the equation $\Delta\Delta G = \Delta T_m \Delta S$, where $\Delta S = 274 \pm 12$ cal/(deg mol) as detailed by Zhang et al. (1991). A positive $\Delta\Delta G$ indicates that the given mutant protein is more stable than the corresponding Ala mutant protein.

Molecular Dynamics. All structures were model built using the coordinates for the wt structure from the Brookhaven Protein Data Bank (Weaver & Matthews, 1987). All structures underwent restrained minimization and 50 ps of restrained molecular dynamics to equilibrate the crystal structure before starting 50 ps of full MD. Simulations were performed with Amber 4 [David A. Pearlman et al. (1991) AMBER 4.0, University of California, San Francisco] and an all-atom force field (Weiner et al., 1986). A 2.0-fs time step and a constant dielectric were used. Bond lengths were constrained with SHAKE (Gunsteren & Berendsen, 1977). Data were collected every 1 ps, and average structures were calculated. The mobile zone for site 44 mutants contained amino acids 36–51 and a 17-Å cap of water centered on 44 CA. For site 68 mutants, the mobile zone contained amino acids 60–80 and 1–5 and a 19-Å cap of water centered on 70 CA. Amino acids 1–5 were included for site 68 because Phe 4 was found to pack against residue 68 in simulations with a mobile zone of residues 60–80 and a 17-Å cap of waters centered on 70 CA.

RESULTS AND DISCUSSION

In order to gain increased insight into the effects of β-branching on α-helix and protein stability, a series of straight-chain and β-branched amino acids (Figure 1) were substituted into two solvent-exposed α-helical positions in T4 lysozyme (T4L). T4 lysozyme was chosen as a model protein since T4L's structure and activity are well characterized (Remington et al., 1978; Tsugita, 1971; Weaver et al., 1987); the stabilities of the wild-type protein and of many mutant proteins have been determined and examined thoroughly (Matthews, 1993); and a wide variety of unnatural amino acids have been incorporated into T4 lysozyme previously (Ellman et al., 1992b,c; Mendel et al., 1991, 1992, 1993). A cysteine-free form of T4L, in which Cys 54 and Cys 97 have been replaced by Thr and Ala, respectively, was used for these experiments as the cysteines have been shown to complicate thermal denaturation experiments and yet to be unnecessary structurally and catalytically (Perry & Wetzel, 1987). Two distinct, but structurally similar, α-helical sites, Ser 44 and Asn 68, were chosen for this study (Remington et al., 1978; Weaver et al., 1987). Both sites lie in the middle of α-helices—helix 39–50 and helix 60–80, respectively—and so should avoid any complications caused by N-cap and C-cap effects. In addition, both sites are between 50% and 60% solvent exposed and so should minimize disruptions due to tertiary packing interactions. There are differences, however, between the two helices. One helix is almost twice as long as the other, and helix 39–50 lies against several β-sheets, whereas helix 60–80 lies between the N- and C-terminal domains of the protein and has more extensive tertiary contacts with the rest of the protein than does helix 39–50.

Measurement of Protein Stabilities. Mutant proteins containing the amino acids alanine, L-2-aminobutanoic acid, valine, L-2-aminopentanoic acid, L-2-amino-3,3-dimethylbutanoic acid, and L-2-aminohexanoic acid (Figure 1) at site Ser 44 or at site Asn 68 in T4 lysozyme were prepared using unnatural amino acid mutagenesis. The mutant proteins were synthesized *in vitro* by suppressing an amber nonsense codon at site 44 or at site 68 in the T4L gene with a suppressor tRNA chemically aminoacylated with the desired amino acid (Bain et al., 1989; Ellman et al., 1992a; Noren et al., 1989). For both sites, the amount of protein produced when the aminoacyl-tRNA was replaced by an unacylated tRNA (the level of readthrough) was determined to be less than 1%. This control ensures that the protein produced by suppressing the amber codon is homogeneous. Suppression efficiencies for the amino acids were judged to be 30% for Ala, 70% for AHA, and 50% for ADBA at site 44 and 30% for Ala, 50% for AHA, and 30% for ADBA at site 68 on the basis of the catalytic activity and protein expression levels (Cornish et al., 1994). The low efficiency for Ala compared to AHA is consistent with previous reports that amino acids with large hydrophobic side chains bind to the *Escherichia coli* elongation factor Tu more tightly than do those with small hydrophobic side chains (Louie & Jurnak, 1984). The lower efficiency of ADBA relative to AHA may be analogous to solid-phase peptide synthesis where the sterically hindered amino acid ADBA has been observed to couple more slowly than other amino acids (Lyu et al., 1991).

The stabilities of mutant T4 lysozymes containing the series of straight-chain and β-branched amino acids (Figure 1) substituted at site 44 or at site 68 were examined initially by a heat of inactivation assay (Matthews et al., 1987; Wells et al., 1986; Streisinger, 1968). For each protein, agreement between the catalytic activity as measured by the rate of lysis of NAP IV cells and the quantity of protein as determined from SDS–PAGE and autoradiography was used to verify the structural integrity of the protein. Using the supernatants of the crude *in vitro* reactions, the loss of T4 lysozyme activity as a function of temperature was determined for each mutant protein by measuring the rate of lysis of NAP IV cells (Figure 2). Since the mean error in the T_m measurements was 0.3 °C using this assay, only changes in T_m greater than 1 °C are considered to be significant. At site 44, only the amino acid ADBA destabilized T4L enough for detection; the T_m of the Ser 44 → ADBA mutant appeared to be ca. 2 °C less than that of the wt protein. At site 68, however, none of the amino acids caused a measurable change in T4 lysozyme's stability. Thus, while the ADBA side chain was destabilizing at site 44, the same side chain at site 68 had little effect on protein stability (Figure 2).

In order to examine the discrepancy between the effect of incorporating a β-branched amino acid at site 44 and that at site 68, the mutant proteins Ser 44 → Ala, Ser → AHA, Ser 44 → ADBA, Asn 68 → Ala, Asn 68 → AHA, and Asn 68 → ADBA were examined more closely. Mutant proteins containing AHA and ADBA were prepared from 10-mL *in vitro* transcription/translation reactions by suppressing an amber codon at site 44 or 68 with a suppressor tRNA charged with the appropriate amino acid. The mutant proteins Ser 44 → Ala and Asn 68 → Ala and the wild-type protein were

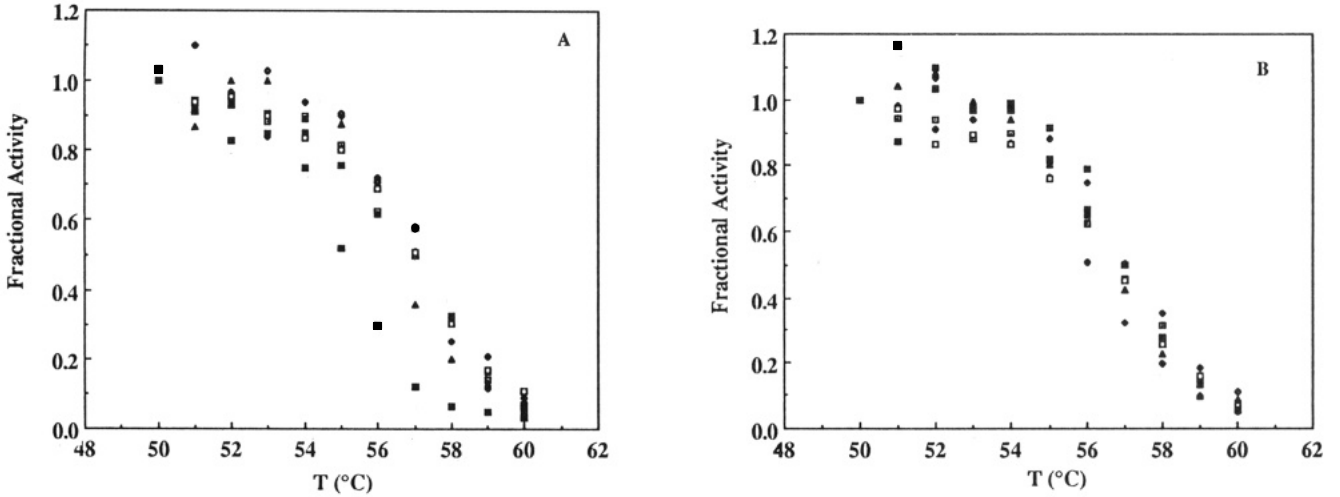

FIGURE 2: Heat of inactivation assays at sites Ser 44 (A) and Asn 68 (B). The stability of each mutant protein is measured from a plot of the residual activity of the protein as a function of temperature (Ellman et al., 1992). The data in this figure represent the average of three measurements. Data are shown for the wild-type (⊡), wt → Ala (◆), wt → ABA (solid square with open dot), wt → Val (◇), wt → ADBA (■), wt → APA (□), and wt → AHA (▲) proteins.

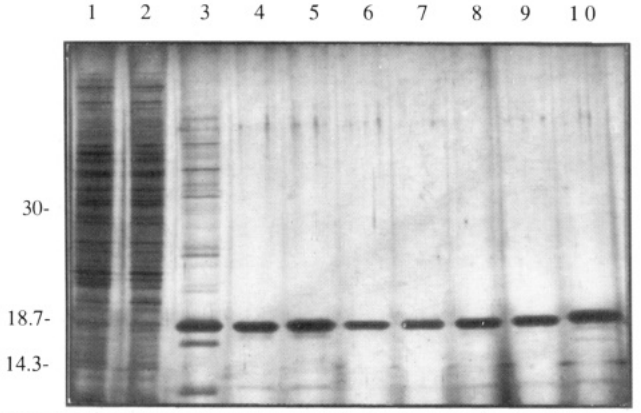

FIGURE 3: Silver-stained 15% SDS–PAGE showing the purification of the *in vitro* synthesized wild-type and mutant T4Ls: lanes 1–3, the crude *in vitro* reaction mixture, the PEI-HCl supernatant, and the combined DEAE-CM-purified fractions, respectively, from the purification of wt T4L; lane 4, purified wt T4L; lane 5, purified Ser 44 → Ala; lane 6, purified Ser 44 → AHA; lane 7, purified Ser 44 → ADBA; lane 8, purified Asn 68 → Ala; lane 9, purified Asn 68 → AHA; lane 10, purified Asn 68 → ADBA.

prepared from 5-mL *in vitro* reactions using plasmids encoding their respective sequences. The proteins were purified by elution from a CM cartridge followed by elution from a Mono S column as described (Cornish et al., 1994). Each protein was judged to be >98% pure on the basis of SDS–PAGE with silver staining (Figure 3). Each protein was dialyzed extensively against a 20 mM potassium phosphate and 25 mM KCl, pH 2.5, buffer. The structural integrity of each mutant protein was verified by comparing the CD spectrum from 200 to 260 nm with that of the wild-type protein. The CD spectra for all mutant proteins were similar to that of wild-type and exhibited minima at 209 and 223 nm (data not shown). The stabilities of the proteins then were determined from the midpoint of their reversible thermal denaturation curves as monitored by circular dichroism with the use of the two-state denaturation model (Table 1) (Beckel et al., 1987).

Impact of Local Context on the Effect of a Mutation. The results of the thermal denaturation experiments clearly demonstrate that the effect of β-branching is dependent on the context of the local helical environment. The Ser 44 → ADBA mutant is 2.5 ± 0.1 °C (0.69 ± 0.03 kcal/mol) less stable than the Ser 44 → Ala mutant, but the Asn 68 → ADBA mutant is 1.0 ± 0.1 °C (0.27 ± 0.03 kcal/mol) more stable than the Asn 68 → Ala mutant (Table 1). The relative stabilities of the mutant proteins as determined from the thermal denaturation curves and by the heat of inactivation assay are similar. Differences in the absolute T_ms as determined by these two methods likely reflect the fact that the thermal denaturation was done at pH 2.5 while the heat of inactivation assay was performed at pH 6.5. The role of the surrounding environment on the effect of an amino acid substitution can also be seen in previous work (Serrano et al., 1992a; Zhou et al., 1993). A comparison of the relative stabilities of different amino acids in α-helices in the proteins T4 lysozyme and barnase and in several model α-helices also reveals context effects (Table 2) (Blaber et al., 1993; Serrano et al., 1992b). In T4 lysozyme, the Ala 44 mutant is 0.33 kcal/mol more stable than the Val 44 mutant; however, in barnase, the Ala 32 mutant is 0.88 kcal/mol more stable than the Val 32 mutant. Given that the range of stabilities seen for all of the natural amino acids, except Pro, at both sites is less than 1.0 kcal/mol, this difference is significant. Even the order of stability of the natural amino acids depends on context; leucine is more stable than isoleucine at site 44 in T4 lysozyme, but isoleucine is more stable at site 131 in the same protein (Blaber et al., 1993).

Table 1: Thermodynamic Stabilities of the T4 Lysozyme Mutants

protein	T_m (°C)[a]	ΔT_m (°C)[b]	$\Delta\Delta G$ (kcal/mol)[b,c]
Ser 44 (wt)	47.8 ± 0.1	−1.6 ± 0.1	−0.44 ± 0.03
Ser 44 → Ala	49.4 ± 0.1		
Ser 44 → AHA	49.2 ± 0.1	−0.2 ± 0.1	0.05 ± 0.03
Ser 44 → ADBA	46.9 ± 0.1	−2.5 ± 0.1	−0.69 ± 0.03
Asn 68 (wt)	47.8 ± 0.1	−0.2 ± 0.1	−0.05 ± 0.03
Asn 68 → Ala	48.0 ± 0.1		
Asn 68 → AHA	48.1 ± 0.1	0.1 ± 0.1	0.03 ± 0.03
Asn 68 → ADBA	49.0 ± 0.1	1.0 ± 0.1	0.27 ± 0.03

[a] The T_m's were determined from the circular dichroism melting curves in duplicate. The error estimates for the T_m's correspond to the standard deviation between the two T_m measurements. [b] The ΔT_m and $\Delta\Delta G$ are reported relative to Ala at the given site. The $\Delta T_m = T_{m,mutant} - T_{m,Ala}$. [c] $\Delta\Delta G = \Delta T_m \Delta S$, where ΔS is assumed to be constant for all mutants with a value of 274 ± 12 cal/(deg mol) (Zhang et al., 1991). A positive $\Delta\Delta G$ indicates that the mutant protein is more stable than the wild-type protein.

Molecular Dynamics Simulations. In order to better understand the factors that influence the stabilities of these T4L mutants, the structures of the proteins were modeled using molecular dynamics simulations (Table 3 and Figure

Table 2: Effect of β-Branched Amino Acids in Different Model Systems

	ΔΔG (kcal/mol)[a]					% helix[g]
amino acid	T4L Ser 44[b]	T4L Val 131[b]	barnase Ala 32[c]	model peptide[d]	model peptide[e]	model peptide[f]
Ala	0.96	0.94	0.91	0.77	0.79 (85%)[g]	78
Val	0.63	0.69	0.03	0.14	0.34 (50%)	17
Ala–Val	0.33	0.25	0.88	0.63	0.45 (35%)	61
Leu	0.92	0.77	0.56	0.62	0.62 (75%)	80
Ile	0.84	0.84	0.10	0.23	0.39 (56%)	41

[a] The protein and peptide stabilities are reported as ΔΔG in kcal/mol, where $\Delta\Delta G = \Delta G_{Gly} - \Delta G_{mutant}$ such that a positive ΔΔG indicates that the substitution is more stable than Gly. Excluding Pro, values for ΔΔG for the 20 natural amino acids range from 0 to 1.0 kcal/mol. [b] Blaber et al., 1993; Blaber et al., 1994. [c] Serrano et al., 1992b. [d] O'Neil & DeGrado, 1990. [e] Lyu et al., 1990. [f] Padmanabhan et al., 1990. [g] The percent helical content of the peptide when three residues in the peptide are the given amino acid. The value for 100% helix was determined from the maximum value for $-[\theta]_{222}$ given by trifluoroethanol titration.

Table 3: Molecular Dynamics Simulations

	native	Ala	AHA	ADBA
site 44				
dihedral angles (deg)				
φ	−60 (−63)[a]	−61 (−65)	−62	−70
ψ	−44 (−51)	−45 (−41)	−46	−35
Lys 43 χ_1	−63 (−84)	−66 (−91)	−74	−176
44 χ_1	−56 (−175)		−75	+62
hydrogen bonds (Å)				
40 O[b]–44 N[b]	3.29 (3.12)	3.47 (2.88)	3.25	3.62
41 O–45 N	3.03 (3.20)	3.14 (3.01)	3.01	3.23
steric clashes (Å)				
44 CG1[c]–41 O				3.37
44 CG1–40 O				3.94
site 68				
dihedral angles				
φ	−54 (−59)	−54	−54	−61
ψ	−49 (−43)	−50	−47	−38
Phe 4 χ_1	−61 (−66)	−59	−51	−53
68 χ_1	−177 (−76)		−70	+63
hydrogen bonds (Å)				
64 O–68 N	3.10 (2.96)	3.10	3.06	3.52
65 O–69 N	3.14 (3.03)	3.30	3.47	3.32
steric clashes (Å)				
68 CG1–65 O				3.42
68 CG1–64 O				3.71

[a] Values in parentheses are those determined by X-ray crystallography (Weaver & Matthews, 1987; Blaber et al., 1994). Differences between the structures found by the MD simulations and by X-ray crystallography may reflect differences between the environment of a constant dielectric with explicit water molecules used for the simulations and that of the protein crystal. [b] O is defined as the backbone carbonyl oxygen; N, as the backbone amide nitrogen. [c] CG1 is defined as the γ-carbon in the g^+ position.

4). Substitution at site 44 with ADBA appears to cause a local disruption in the α-helix. In order to minimize close contacts between the g^+ γ-methyl group of the *tert*-butyl side chain and the backbone oxygens of residues Ala 41 (average distance 3.37 Å) and Asn 40 (average distance 3.94 Å) (Figure 4A), the dihedral angles at site 44 change and the local backbone hydrogen bonds lengthen. The φ value of residue 44 changes from −60 ° in the wild-type structure to −70° in the mutant structure, and the ψ value changes from −44 ° to −35°. The hydrogen bond between the carbonyl oxygen of Asn 40 and the backbone NH group of residue 44 increases from 3.29 Å in the native structure to 3.62 Å in the mutant structure. Similarly, the hydrogen bond between the Ala 41 carbonyl oxygen and Glu 45 NH group increases from 3.03 to 3.23 Å. In contrast, neither the Ser 44 → AHA nor the Ser 44 → Ala mutant appears to cause such a disruption in the α-helix. Several potential side-chain packing interactions are seen in the Ser 44 and the Ser 44 → Ala, AHA, and ADBA structures. Most significant is a packing interaction between the side chains of Lys 43 and ADBA 44 (Figure 4B) that is absent in the Ser 44 → Ala mutant. Based on the MD simulations, the Ser 44 → ADBA mutant buries 22 Å^2 more hydrophobic surface area than the Ser 44 → Ala mutant. Two caveats to this interpretation of the side-chain packing interactions, however, are (i) Lys 43 can potentially form van der Waals contacts with Leu 39 in the wt, Ser 44 → Ala, and Ser 44 → AHA structures (Figure 4C) such that the net gain in buried hydrophobic surface area for the ADBA mutant may be significantly less than 22 Å^2 and (ii) in contrast to free energy perturbation calculations (Hermans et al., 1992), these simulations do not provide an estimate of the entropic cost of side-chain packing. In solution, it is reasonable to expect that the side chains of solvent-exposed residues are dynamic and, therefore, that the loss of side-chain entropy upon packing may be significant.

Similar results are seen at site Asn 68 (Table 3 and Figure 4). For the Asn 68 → ADBA mutant, the φ value of residue 68 changes from −54° to −61°, and the ψ value changes from −49° to −38°. The hydrogen bond between the carbonyl oxygen of Glu 64 and the NH group of Asn 68 lengthens from 3.10 to 3.52 Å, and that between the Lys 65 carbonyl oxygen and the Gln 69 NH group lengthens from 3.14 to 3.47 Å. The local helical structure is not perturbed significantly in the Asn 68 → Ala or Asn 68 → AHA structure. Several potential side-chain packing interactions are again observed: the ADBA side chain packs against Phe 4, which is constrained about χ_1, such that the Asn 68 → ADBA mutant (Figure 4D) buries 23 Å^2 more surface area than does the Asn 68 → Ala mutant. The AHA side chain packs against the Lys 65 side chain in the Asn 68 → AHA mutant (Figure 4E), but as discussed above, the MD simulations do not account for the entropic cost expected for such an interaction.

Effects of β-Branched Amino Acids on α-Helix Stability. One explanation for the destabilizing effect of β-branched amino acids such as Val is the loss in side-chain conformational entropy upon α-helix formation. A correlation has been proposed between the loss in side-chain entropy upon α-helix formation and the helix-forming propensities of the 20 natural amino acids (Blaber et al., 1994; Creamer & Rose, 1992). For the β-branched amino acids, there is a considerable loss in side-chain entropy upon α-helix formation because χ_1 is restricted to one (tg^-)[1] of three possible rotamers (Nemethy et al., 1966; Piela et al., 1987). In an α-helix, the g^+ rotamer is disfavored energetically because of steric repulsion by the $i-3$ and $i-4$ carbonyl oxygens in the preceding turn of the helix (see Figure 4A). This entropic factor does not account for the destabilization caused by ADBA, however, as ADBA has only one low-energy rotamer, the staggered conformation. Rather, ADBA may destabilize α-helices because one of the γ-methyl groups of ADBA must occupy the disfavored g^+ position. Hermans and co-workers estimated the energetic cost of incorporating ADBA into a poly(Ala) α-helix to be about 1.2 kcal/mol on the basis of the theoretical free energies of the three side-chain rotamers of L-2-aminobutanoic acid (Hermans et al., 1992). In addition, both Val and ADBA would be expected to destabilize α-helices on the basis of theoretical calculations of the conformational space available to the capped amino acids (Nemethy et al., 1966; Paterson & Leach, 1978). Both amino acids have limited conformational

[1] The nomenclature used throughout this paper for χ_1 rotamers is according to Ponder and Richards (1987). Please note that this nomenclature is different from that used by McGregor et al. (1987).

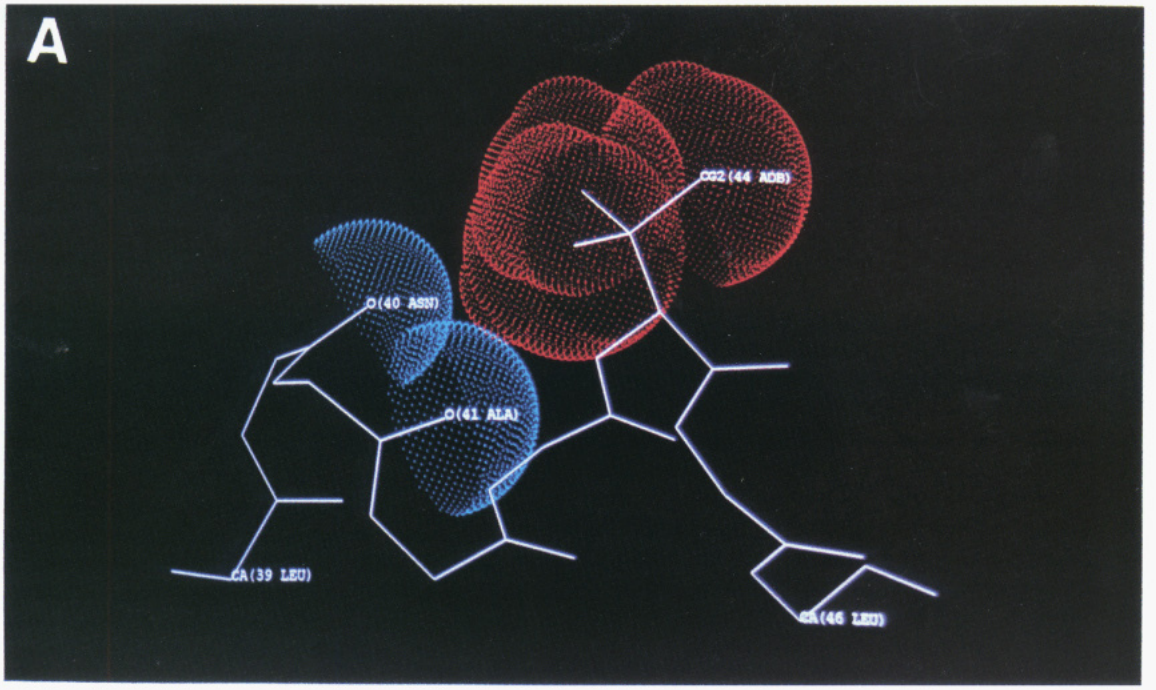
A
CG2 (44 ADB)
O (40 ASN)
O (41 ALA)
CA (39 LEU)
CA (46 LEU)

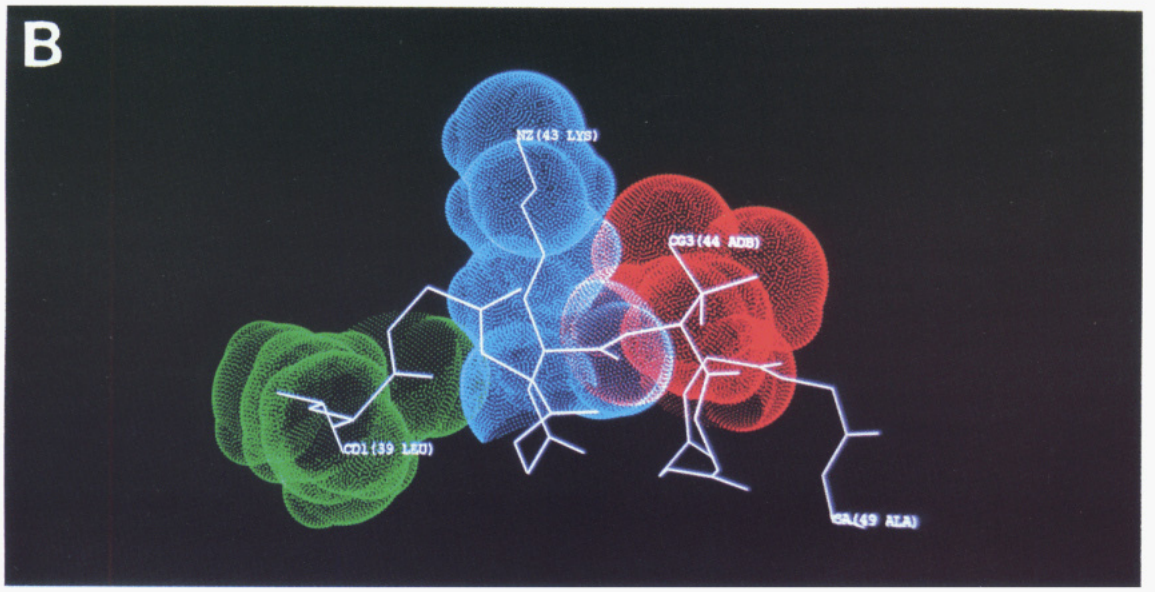
B
NZ (43 LYS)
CG3 (44 ADB)
CD1 (39 LEU)
CA (49 ALA)

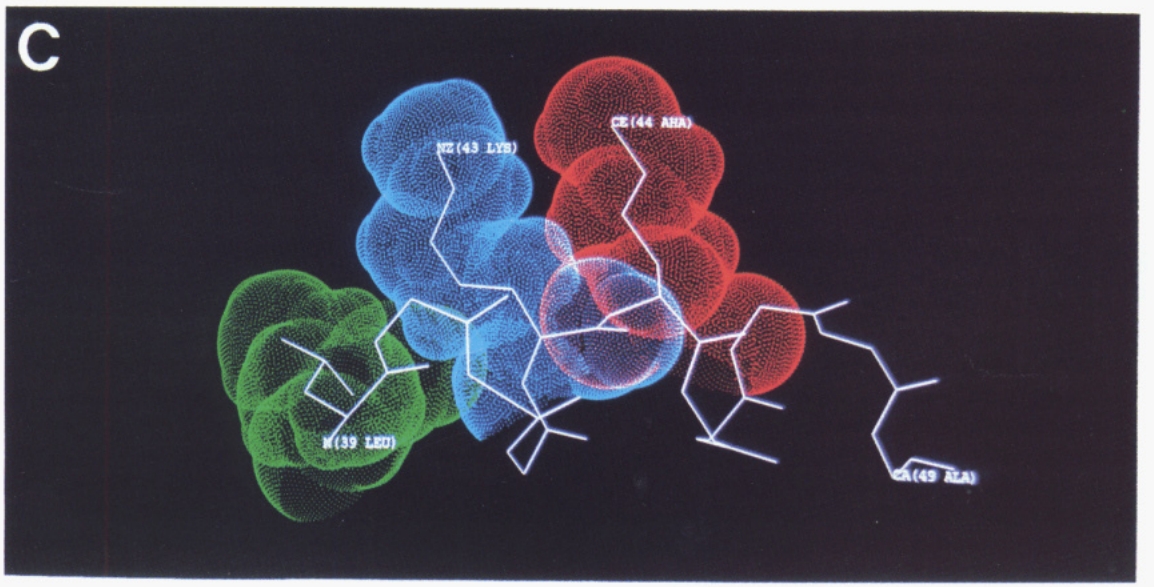
C
CE (44 AHA)
NZ (43 LYS)
N (39 LEU)
CA (49 ALA)

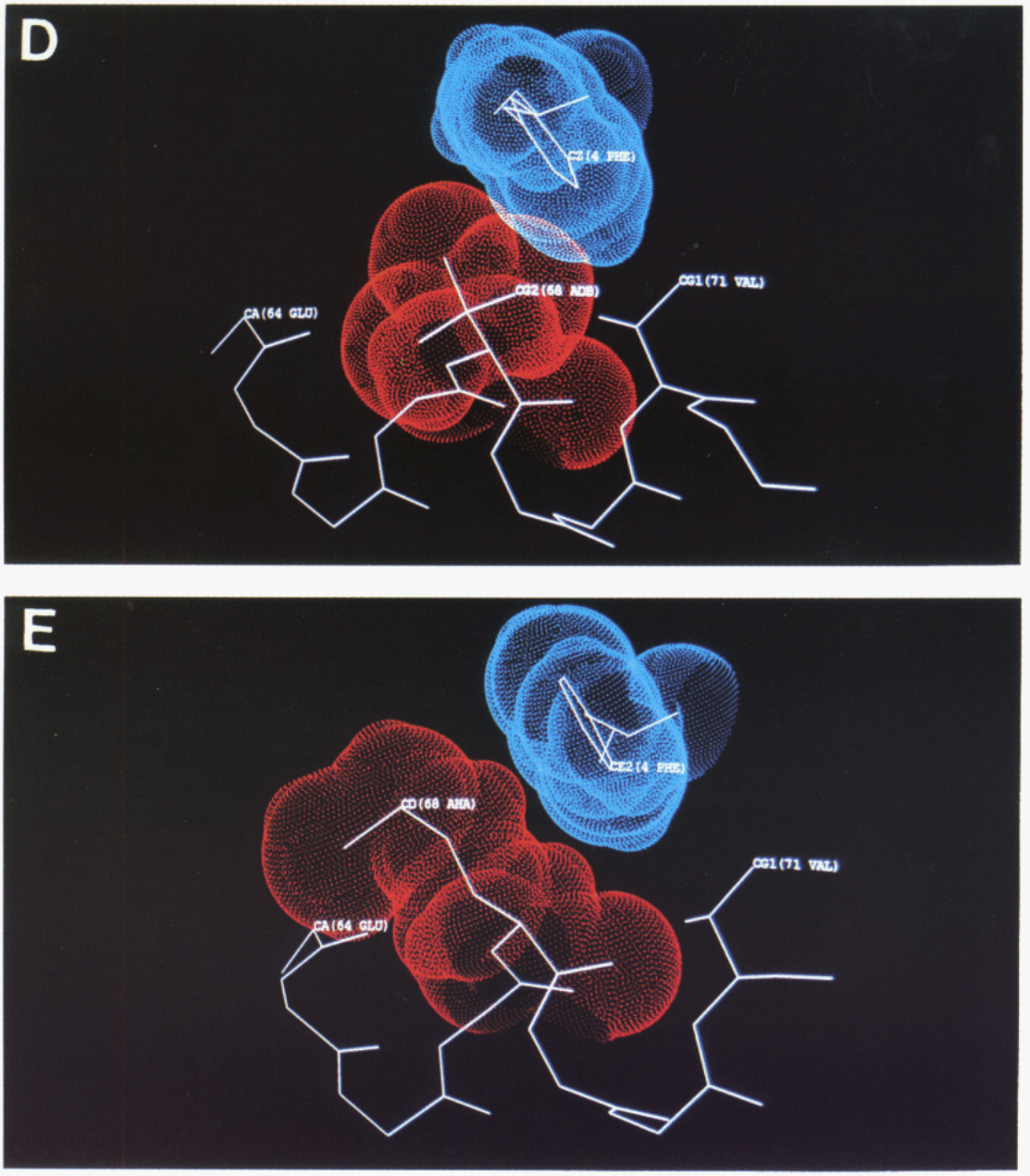

FIGURE 4: Graphic representations of the site 44 and site 68 mutant structures as determined from MD simulations. The areas shown in color correspond to the van der Waals radii of the given atoms. (A) In the Ser 44 → ADBA mutant, the van der Waals surface of the ADBA side chain (red) overlaps with that of the carbonyl oxygens (blue) of Asn 40 and Ala 41. A similar interaction is seen in the Asn 68 → ADBA mutant. (B) In the Ser 44 → ADBA mutant, the side chain of ADBA (red) packs against the side chain of Lys 43 (blue), while the side chain of Leu 39 (green) is solvent exposed. (C) In the Ser 44 → AHA mutant, however, the side chain of AHA (red) is solvent exposed, while the side chain of Leu 39 (green) packs against that of Lys 43 (blue). (D) In the Asn 68 → ADBA mutant, the side chain of ADBA (red) packs against the side chain of Phe 4 (blue). (E) In the Asn 68 → AHA mutant, the AHA side chain (red) does not appear to bury as much hydrophobic surface area against the side chain of Phe 4 (blue) as does ADBA. Note that in these graphics the ADBA side chain is labeled ADB.

freedom, and their ϕ/ψ minima lie outside of the ϕ/ψ region for a right-handed α-helix. In accordance with these theoretical calculations, MD calculations indicate that the ADBA side chain causes disruptions in the local helix backbone at both sites 44 and 68 (Table 3). The ADBA side-chain γ-methyl group that occupies the g^+ position clearly comes into steric contact with the carbonyl oxygens of the residues at positions $i-3$ and $i-4$ in the preceding turn of the helix (Figure 4A). To minimize this repulsive interaction, the local helical geometry appears to be distorted at both positions.

In contrast to the destabilizing steric effects, the restriction in rotational freedom imposed by β-branching may improve hydrophobic packing interactions. In general, solvent-exposed residues would have to lose considerable side-chain conformational freedom in order to form van der Waals contacts with other surface residues. For the β-branched amino acids ADBA and Val, which are constrained to one χ_1 rotamer in an α-helix, side-chain packing may be more favorable entropically than for unbranched amino acids such as AHA and Lys. This effect is consistent with the increased stability of the Asn 68 → ADBA relative to the Asn 68 → AHA mutant. Moreover, the observed experimental stabilities of the Asn 68 → ADBA and Ser 44 → ADBA mutants may reflect the fact that at site 68 the ADBA side chain packs against a relatively immobile Phe side chain, whereas at site 44 the ADBA side chain packs against a conformationally unconstrained Lys side chain. The energetic cost of the loss of side-chain entropy was illustrated also in a previous study in which unnatural

amino acids were designed to stabilize T4L by filling a hydrophobic cavity in the protein (Mendel et al., 1992).

Comparison with Previous Studies of Protein and Peptide α-Helix Stability. At both positions, the Ala and AHA mutants are relatively close in stability to one another. This result is consistent with that seen in model peptides (Lyu et al., 1991; Padmanabhan & Baldwin, 1991). Assuming that the AHA side chain projects out into solvent, it would not bury significantly more surface area against the helix core than would the Ala side chain. Packing of the AHA side chain against neighboring side chains may not be very stabilizing, as noted above, because of a concomitant loss in side-chain entropy. For example, if only 1 of the 27 rotamers of AHA can form a stabilizing contact in the native protein and 10 are energetically allowed in the denatured protein, a hydrophobic contact would have to be worth 1.4 kcal/mol just to compensate for the entropic destabilization. The Ser 44 → Ala mutation is slightly stabilizing, as is expected for a solvent-exposed Ser to Ala mutation in an α-helix (Blaber et al., 1993). The Asn 68 → Ala mutation is less stabilizing than would be expected. Asn has been proposed to destabilize helices because the side chain can form a six-membered hydrogen bond to the amide backbone in the denatured state (Horovitz et al., 1992).

Given the impact of local context on the effect on protein stability of placing a β-branched amino acid in an α-helix, it is not possible to compare the magnitude of the effect of β-branching on α-helix stability in an isolated peptide to that in a protein. Interestingly, however, the effect of β-branched amino acids on helix stability at site 44 in T4L is similar to that in the model α-helical peptide studied by Lyu et al. At site 44, Ala is about 0.3 kcal/mol more stable than Val (Blaber et al., 1993) and about 0.7 kcal/mol more stable than ADBA. In the model helix of Lyu et al., Ala is about 0.45 kcal/mol more stable than Val and about 0.9 kcal/mol more stable than ADBA. It is interesting that in both cases the amino acid bearing a *tert*-butyl side chain is twice as destabilizing as the amino acid bearing an isopropyl side chain. As discussed above, the *tert*-butyl side chain has been proposed to be destabilizing because of steric repulsion with the preceding turn of the helix, whereas the isopropyl side chain has been proposed to be destabilizing because of a loss in side-chain entropy. More work is needed to determine the magnitude of destabilization or stabilization which can be caused by β-branched amino acids and to assess the generality of the stabilization seen at site Asn 68 for the ADBA mutation.

Conclusion. In trying to understand protein stability and protein folding pathways, it is tempting to assign values to different factors, such as β-branching, which impact protein structure. These values, however, do not account for the variations observed in the thermal stabilities of the mutant proteins described here. Incorporation of ADBA, which had been expected to be very destabilizing, at two apparently similar α-helical sites in the same protein results in opposite effects. At site Ser 44 the ADBA substitution *destabilizes* T4 lysozyme by 2.5 ± 0.1 °C (0.69 ± 0.03 kcal/mol) relative to the Ala substitution; at site Asn 68 the ADBA substitution *stabilizes* T4 lysozyme by 1.0 ± 0.1 °C (0.27 ± 0.3 kcal/mol) relative to the Ala substitution (Table 1). Molecular dynamics simulations suggest that ADBA leads to disruption of the helix at both sites 44 and 68 but that ADBA can form stabilizing hydrophobic packing interactions at both sites (Table 3 and Figure 4). It is proposed that ADBA is stabilizing at site 68 because of a particularly favorable van der Waals interaction between the ADBA 68 and Phe 4 side chains. In addition to demonstrating the influence of local context effects, these results give insight into the potential impacts of β-branching. β-Branching restricts the rotational freedom of an amino acid side chain, which can, in turn, destabilize an α-helix because the β-branched amino acids and the surrounding amino acids in the α-helix must adopt energetically disfavored torsion angles. At the same time, however, this restriction may improve side-chain van der Waals interactions because there it reduces the entropic cost of packing the side chain against other residues.

ACKNOWLEDGMENT

The authors thank Professor S. Marqusee (University of California, Berkeley) for advice concerning the CD thermal denaturation experiments and for helpful discussions.

REFERENCES

Bain, J. D., Glabe, C. G., Dix, T. A., Chamberlin, A. R., & Diala, E. S. (1989) *J. Am. Chem. Soc. 111*, 8013–8014.
Becktel, W. J., & Baase, W. A. (1987) *Biopolymers 26*, 619–623.
Blaber, M., Zhang, X.-J., & Matthews, B. W. (1993) *Science 260*, 1637–1640.
Blaber, M., Zhang, X. J., Lindstrom, J. D., Deprot, S. D., Baase, W. A., & Matthews, B. W. (1994) *J. Mol. Biol. 235*, 600–624.
Chou, P. Y., & Fasman, G. D. (1978) *Annu. Rev. Biochem. 47*, 251–276.
Cornish, V. W., Benson, D. R., Altenbach, C. A., Hideg, K., Hubbell, W. L., & Schultz, P. G. (1994) *Proc. Natl. Acad. Sci. U.S.A. 91*, 2910–2914.
Creamer, T. P., & Rose, C. D. (1992) *Proc. Natl. Acad. Sci. U.S.A. 89*, 5937–5941.
Creighton, T. E. (1990) *Biochem. J. 270*, 1–16.
Dill, K. A. (1990) *Biochemistry 29*, 7133–7155.
Ellman, J. A., Mendel, D., Anthony-Cahill, S., Noren, C. J., & Schultz, P. G. (1992a) *Methods Enzymol. 202*, 301–336.
Ellman, J. A., Mendel, D., & Schultz, P. G. (1992b) *Science 255*, 197–200.
Ellman, J. A., Volkman, B. F., Mendel, D., Schulz, P. G., & Wemmer, D. E. (1992c) *J. Am. Chem. Soc. 114*, 7959–7961.
Gunsteren, W. F. v., & Berendsen, H. J. C. (1977) *Mol. Phys. 34*, 131.
Hermans, J., Anderson, A. G., & Yun, R. H. (1992) *Biochemistry 31*, 5646–5653.
Horovitz, A., Matthews, J. M., & Fersht, A. R. (1992) *J. Mol. Biol. 227*, 560–568.
Kim, P. S., & Baldwin, R. L. (1990) *Annu. Rev. Biochem. 59*, 631–660.
Kutamura, S., & Sturtevant, J. M. (1989) *Biochemistry 28*, 3788–3797.
Louie, A., & Jurnak, F. (1985) *Biochemistry 24*, 6433–6439.
Lyu, P. C., Liff, M. I., Marky, L. A., & Kallenbach, N. R. (1990) *Proc. Natl. Acad. Sci. U.S.A. 250*, 669–673.
Lyu, P. C., Sherman, J. C., Chen, A., & Kallenbach, N. R. (1991) *Proc. Natl. Acad. Sci. U.S.A. 88*, 5317–5320.
Marqusee, S., Robbins, V. H., & Baldwin, R. L. (1989) *Proc. Natl. Acad. Sci. U.S.A. 86*, 5286–5290.
Matthews, B. W. (1993) *Annu. Rev. Biochem. 62*, 139–160.
Matthews, B. W., Nicholson, H., & Becktel, W. J. (1987) *Proc. Natl. Acad. Sci. U.S.A. 84*, 6663–6667.
McGregor, M. J., Islam, S. A., & Sternberg, M. J. E. (1987) *J. Mol. Biol. 198*, 295–310.
Mendel, D., Ellman, J. A., & Schultz, P. G. (1991) *J. Am. Chem. Soc. 113*, 2758–2760.
Mendel, D., Ellman, J. A., Chang, Z., Veenstra, D. L., Kollman, P. A., & Schultz, P. G. (1992) *Science 256*, 1798–1802.
Mendel, D., Ellman, J., & Schultz, P. G. (1993) *J. Am. Chem. Soc. 115*, 4359–4360.

Merutka, G., Lipton, W., Shalongo, W., Park, S.-H., & Stellwagen, E. (1990) *Biochemistry 29*, 7511–7515.
Nemethy, G., Leach, S. J., & Scheraga, H. A. (1966) *J. Phys. Chem. 70*, 998–1004.
Noren, C. J., Anthony-Cahill, S. J., Griffith, M. C., & Schultz, P. G. (1989) *Science 244*, 182–188.
O'Neil, K. T., & DeGrado, W. F. (1990) *Science 250*, 646–651.
Padmanabhan, S., & Baldwin, R. L. (1991) *J. Mol. Biol. 219*, 135–137.
Padmanabhan, S., Marqusee, S., Ridgeway, T., Laue, T. M., & Baldwin, R. L. (1990) *Nature 344*, 268–270.
Paterson, Y., & Leach, S. J. (1978) *Macromolecules 11*, 409–415.
Perry, L. J., & Wetzel, R. (1986) *Biochemistry 25*, 733–739.
Perry, L. J., & Wetzel, R. (1987) *Protein Eng. 1*, 101–105.
Piela, L., Nemethy, G., & Scheraga, H. A. (1987) *Biopolymers 26*, 1273–1286.
Ponder, J. W., & Richards, F. M. (1987) *J. Mol. Biol. 193*, 775–791.
Remington, S. J., Anderson, W. F., Owen, J., Eyck, L. F. T., Grainger, C. T., & Matthews, B. W. (1978) *J. Mol. Biol. 118*, 81–98.
Richardson, J. S., & Richardson, D. C. (1988) *Science 240*, 1648–1652.
Robertson, S. A., Ellman, J. A., & Schultz, P. G. (1991) *J. Am. Chem. Soc. 113*, 2722–2729.
Sanger, F., Nicklen, S., & Caulson, A. R. (1977) *Proc. Natl. Acad. Sci. U.S.A. 74*, 5463–5467.
Santoro, M. M., & Bolen, D. W. (1992) *Biochemistry 31*, 4901–4917.
Sayers, J. R., Schmidt, W., & Eckstein, F. (1988) *Nucleic Acids Res. 16*, 791–802.
Scheraga, H. A. (1978) *Pure Appl. Chem. 50*, 315–324.
Scholtz, J. M., Qian, H., York, E. J., Steward, J. M., & Baldwin, R. L. (1991) *Biopolymers 13*, 1463–1470.
Serrano, L., Neira, J.-L., Sancho, J., & Fersht, A. R. (1992a) *Nature 356*, 453–455.
Serrano, L., Sancho, J., Hirshberg, M., & Fersht, A. R. (1992b) *J. Mol. Biol. 227*, 544–559.
Sueki, M., Lee, S., Powers, S. P., Denton, J. B., Konishi, Y., & Scheraga, H. A. (1984) *Macromolecules 17*, 148–155.
Tsugita, A. (1971) in *The Enzymes* (Boyer, P. D., Ed.) pp 343–411, Academic Press, New York.
Tsugita, A., Inouye, M., Terzaghi, E., & Streisinger, G. (1968) *J. Biol. Chem. 243*, 391–397.
Weaver, L. H., & Matthews, B. W. (1987) *J. Mol. Biol. 193*, 189–199.
Weiner, S. J., Kollman, P. A., Nguyen, D. T., & Case, D. A. (1986) *J. Comput. Chem. 7*, 230–252.
Wells, J. A., & Powers, D. B. (1986) *J. Biol. Chem. 261*, 6564–6570.
Williams, R. W., Chang, A., Juretic, D., & Loughran, S. (1987) *Biochim. Biophys. Acta 916*, 200–204.
Wojcik, J., Altmann, K.-H., & Scheraga, H. A. (1990) *Biopolymers 30*, 121–134.
Zhang, X. J., Baase, W. A., & Matthews, B. W. (1991) *Biochemistry 30*, 2012–2017.
Zhou, N. E., Kay, C. M., Sykes, B. D., & Hodges, R. S. (1993) *Biochemistry 32*, 6190–6197.
Zimm, B. H., & Bragg, J. K. (1959) *J. Chem. Phys. 31*, 526–535.